Optimization of a fedbatch bioreactor for 1,3-propanediol production using hybrid nonlinear optimal control

Jianxiong Ye[a,b,*], Honglei Xu[a,c,*], Enmin Feng[d], Zhilong Xiu[e]

[a]*School of Energy and Power Engineering, Huazhong University of Science and Technology, Wuhan, Hubei, 430074, China*
[b]*School of Mathematics and Computer Science, Fujian Normal University, Fuzhou, Fujian, 350108, China*
[c]*Department of Mathematics and Statistics, Curtin University, Perth, 6845, Australia*
[d]*School of Mathematical Sciences, Dalian University of Technology, Dalian, 116024, Liaoning, China*
[e]*Department of Biotechnology, Dalian University of Technology, Dalian, 116012, Liaoning, China*

Abstract

A nonlinear hybrid system was proposed to describe the fed-batch bioconversion of glycerol to 1,3-propanediol with substrate open loop inputs and pH logic control in previous work (Ye et al., 2011). The current work concerns the optimal control of this fed-batch process. We slightly modify the hybrid system to provide a more convenient mathematical description for the optimal control of the fed-batch culture. Taking the feeding instants and the terminal time as decision variables, we formulate an optimal control model with the productivity of 1,3-propanediol as the performance index. Inequality path constraints involved in the optimal control problem are transformed into a group of end-point constraints by introducing an auxiliary hybrid system. The original optimal control problem is associated with a family of approximation problems. The gradients of the cost functional and the end-point constraint functions are derived from the parametric sensitivity system. On this basis, we construct a gradient-based algorithm to solve the approximation problems. Numerical results show that the productivity of 1,3-propanediol can be increased considerably by employing

*Corresponding author: Honglei Xu
Email addresses: jxye@fjnu.edu.cn (Jianxiong Ye), H.Xu@curtin.edu.au (Honglei Xu)

our optimal control policy.

Key words: Optimal control; hybrid system; inequality path constraint; parametric sensitivity system, optimization algorithm

1. Introduction

1,3-Propanediol (1,3-PD) has wide applications for a large volume of markets, especially as a monomer for polyesters, polyethers and polyurethanes (Homann et al, 1990). Generally, 1,3-PD is produced by chemical or biotechnological route. Compared with chemical synthesis, the bioconversion of glycerol to 1,3-PD is more attractive to industry since it is environmentally safe and has renewable feedstock (Zeng et al., 1994). There are three typical cultures for microbial fermentation of glycerol, including batch, continuous and fed-batch cultures, among which the fed-batch fermentation has attracted great interest due to its high productivity (Cheng et al., 2004).

To improve the productivity of the fed-batch culture, the concentration of the substrate should be controlled in a proper level. In the laboratory, the addition of the substrate is determined by a preassigned sequence of feeding times, which is usually given on an empirical basis. With consideration of expensive cost, it is impossible to carry out plenty of experiments under various glycerol feeding strategies to obtain the optimal one. For this reason, mathematical modelling and optimal control of this microbial process become necessary.

Over the past decades, model-based optimization of biological processes has been attracted the attention of many scientists and engineers (e.g., Asenjo et al., 1996; Cacik et al., 2001; Banga et al., 2005). Banga et al. (2003) presented an excellent review of various methods for bioreactor optimization. Recently, researchers have also put great effort on multiple objective optimal control of bioprocesses (e.g., Logist, et al., 2009; Mandli et al., 2012; Logist, et al., 2013). Modelling and optimization of glycerol fermentation by *Klebsiella* pneumoniae have been considered by Gao et al., 2006; Wang et al., 2008; Yan et al., 2012; Liu et al., 2011; Wang et al., 2012a, 2012b, 2012c. However, most of the previous researches on this bioprocess only considered the technique with both open loop inputs of glycerol and alkali. Till now, the technique with open loop glycerol inputs and pH logic control is seldom discussed, and the existing theoretical work in this aspect includes the nonlinear hybrid modelling (Ye et al., 2011) and the continued parameter identification in (Ye et al., 2012). Yet optimal control of this bioprocess hasn't been discussed.

To address optimal control problems, there are in general two categories of methods: indirect methods, which are based on solving Pontryagin's necessary conditions (e.g., Bryson and Ho, 1975), and direct method, in which the infinite dimensional optimization problem is reduced to a finite dimensional one by using control parametrization (e.g., Goh and Teo, 1988a) or complete discretization (e.g., Tsang and Himmelblau, 1975; Renfro et al., 1987).

Control parametrization methods (known as sequential methods) have been extensively studied from both theoretical and applied aspects over the past decades. See, for example, Teo and Goh, 1989a; Barton et al., 2000; Barton et al., 2002; Loxton et al., 2009. In control parametrization, only the controls are discretized and the dynamic system is decoupled from the optimization stage. Given initial conditions and a set of control parameters, the dynamic system is solved within an inner loop controlled by an NLP solver, and parameters representing the control variables are updated by the NLP solver itself. One of the advantages of control parametrization scheme is that a good approximation of the state variables can be obtained without affecting the size of the NLP problem. However, if the inequality path constraints are involved, the solution would become much more complicated due to the potential high-index DAEs composed of the active path constraints and the original ODEs or DAEs. To overcome this problem, Feehery and Barton (1998; 1999) have proposed an approach based on the dummy derivatives to deal with high-index DAEs. Other practical methods are included in Chen and Vassiliadis (2005) and the references therein. In general, handling the path constraints by using DAE solver would reduce the number of decision variables in the combined NLP solver, because part of the decision variables may be directly determined in the DAE solver.

Therefore, this method for handling path constraints would be much more efficient than that including the path constraints in the master NLP (Feehery and Barton, 1999).

In complete discretization (known as simultaneous approach) the state variables are discretized at the same level of the control variables. Tsang et al. (1975) used collocation to discretize the dynamic system. Biegler (1984) applied global orthogonal collocation and Lagrange polynomials for the approximation of the continuous variables. An efficient simultaneous solution strategy based on multiple shooting and reduced SQP was proposed by Leineweber et al. (2003a,2003b). An excellent review of simultaneous strategies can be founded in Biegler (2007). The simultaneous approaches have several advantages: firstly, simultaneous approaches directly couple the solution of ODE/DAE system with the optimization problem, the dynamic system needs to be solved only once during the optimization procedure; secondly, simultaneous approaches can deal with instabilities that occur for a range of inputs; thirdly, simultaneous approaches such as multiple shooting method have advantages for singular control problems and problems with high index path constraints. In particular, the simultaneous strategy is the relative ease in handling path constraints by including them directly in the optimization problem as a set of point constraints (Feehery and Barton, 1998). Recent work (Drag and Styczen, 2012) has also shown that the simultaneous approaches have advantages in parallel computing. However, it has been well recognized that the simultaneous approaches lead to large scale NLP that requires efficient optimization strategies (Biegler, 2007).

The optimization of glycerol fed-batch process considered in this work is a dynamic optimization of switching times due to the special control method of this bioprocess. In the laboratory, since it is hard to control the flow rate of glycerol precisely by the pump, the flow rate is set to be a fixed constant and the inlet flow is controlled by on/off switches of the pump. Therefore, the decision variables are the feeding instants and the terminal time, and the considered problem is essentially an optimal parameter selection problem (OPSP) with inequality path constraints arising from biochemical limitations on the system.

It is therefore not necessary to use discretization technique for this problem. In addition, it is not suitable for OPSP to directly handle the path constraints in the DAE solver. The reason is that one often fails to determine part of the decision variables due to the possible over-determination in the DAE system.

In this work, we firstly modify the hybrid system proposed in our previous work (Ye et al., 2011) on the basis of a control method that is much easier to be implemented on the equipment of our laboratory. Then, taking the feeding instants and the terminal time as decision variables, we formulate a free-time optimal control model with the productivity of 1,3-PD as performance index, in which inequality path constraints are involved. An auxiliary state-based impulsive system is introduced to derive the sensitivity functions of the hybrid system with respect to the decision variables, and the inequality path constraints are transformed into a group of end-point constraints. The original optimal control problem is finally associated with a family of approximation ones, parametrized by a tolerance error for the end-point constraints. A gradient-based algorithm is constructed to solve the approximation problem. Numerical results show that the algorithm can solve the optimal control problem efficiently.

This paper is organized as follows. In Section 2, we present the nonlinear hybrid dynamical system of the fed-batch culture and the basic properties of the system. In Section 3, an optimal control model with path constraints is formulated, and the corresponding approximation problems are deduced. Section 4 is devoted to the algorithm of the approximation problems and Section 5 shows the corresponding numerical results. Discussions and conclusions are presented at the end of this paper.

2. Reformulation of the nonlinear hybrid dynamical system in fed-batch culture

The fermentation of glycerol by *Klebsiella* pneumoniae is a complex bioprocess, since microbial growth is subjected to multiple inhibitions of substrate and products (Zeng et al., 1994). Among most of the literature, the considered states are the biomass, the substrate glycerol, the product 1,3-PD, the inhibitory metabolites acetate and ethanol (Zeng et al., 1994; Wang et al., 2008; Wang et al., 2012a). In our previous work (Ye et al., 2011), we introduced two additional states, Na+ ions and the volume of the solution, so as to formulate the logic control of the PH of the solution in the reactor.

In the fed-batch culture, the substrate glycerol is discontinuously added to the reactor every so often in order that glycerol concentration keeps in a given range. Alkali (NaOH solution) is also fed into the reactor from time to time for neutralizing the formed acid byproduct such as acetic acid, lactic acid, succinic acid and so on. The inputs of glycerol and alkali are determined by a preassigned time sequence and a pH logic controller, respectively. The flows of alkali and glycerol are set to be constant rates. According to the above description, the fermentation switches among the following four different operating modes throughout the entire fed-batch process.

Mode 0. batch process (no glycerol or alkali feeding);

Mode 1. semibatch process with alkali feeding only;

Mode 2. semibatch process with feeding glycerol only;

Mode 3. semibatch process with both glycerol and alkali feeding.

Some notations are adopt as follows. Let $[t_0, T]$ be the entire time horizon of the fed-batch fermentation, and let $T_{ad} := [T_*, T^*]$ be the admissible set of T, which is known a prior in the laboratory. Let $x(t) := (x_1(t), x_2(t), \ldots, x_7(t))^\intercal$ be the continuous state vector at time t, the components of which are the concentrations of biomass (g·L^{-1}), glycerol (mmol·L^{-1}), 1,3-PD (mmol·L^{-1}), acetate (mmol·L^{-1}), ethanol (mmol·L^{-1}), Na+ ions (mmol·L^{-1}) coming from the added NaOH and the volume (L) of the solution, respectively. If there is no confusion, we also simplify $x(t)$ as x.

2.1. Mathematical description of glycerol feeding strategy

The input of glycerol is an open-loop control, which, however, takes only discrete values. To formulate this class of control functions, a general framework is to use a set of $N+1$ ordered time points $t_0 = \bar{b}_0 < \bar{b}_1 < \ldots < \bar{b}_N = T$ to divide the entire time horizon into N segments. Then the input signal of glycerol can be represented by the following piecewise constant function

$$F_G(t) = F_G(t; \bar{a}, \bar{b}) = \sum_{i=1}^{N} \chi_{[\bar{b}_{i-1}, \bar{b}_i)}(t)\bar{a}_i, \tag{1}$$

where $\bar{b} = (\bar{b}_0, \bar{b}_1, \bar{b}_2, \cdots, \bar{b}_N)^\intercal$, and $\bar{a} = (\bar{a}_1, \bar{a}_2, \cdots, \bar{a}_N)^\intercal$ composting of the values of inlet flow rate of glycerol in each segment. $\chi_I(t)$ denotes the characteristic function of I. If there is no confusion, we also simplify $F_G(t)$ as F_G.

In the factual experiments, the inlet flow rate of glycerol only takes two discrete values, i.e., $\bar{a}_i \in \{0, F_G^m\}$, where F_G^m is the maximum flow rate of glycerol pump. Since the inlet flow rate of glycerol always takes zero value at the beginning of the experiments, the unknown variables are only the number of switches and the time points b_i, while the input value $\bar{a}_i$ in each segment is fixed. That is, the variables to be optimized are only the integer N and the vector $\bar{b}$. A common method for solving this class of problems is to separately treat the discrete and continuous variables in two different optimization level. For example, Xu and Antsaklis (2002) proposed a two-stage algorithm for solving switching optimal control problems, in which the switching times are optimized in Stage one and the number of switchings as well as the modes are optimized in Stage 2. Egerstedt et al. (2003) proposed a gradient-descent algorithm for solving switching optimal control problem, in which the continuous variables are optimized by using the gradient-based methods, and the number of switching times can be optimized by evaluating the gradients between two adjacent time points and deciding whether to inject a new switching time point or not. The solution methods in this framework would be computationally expensive, because the continuous optimal control subproblem is an expensive step and typically must be performed many times to solve the problem.

For the particular problem considered here, we can see from our previous work (Ye et al., 2011) that the switching number N would be quite large (usually no less than 1000). Therefore, the resulting NLP would also be a large scale one if the control function of glycerol input is expressed as a general form in

(1). On the other hand, even if the resulting NLP can be solved properly, the obtained optimal control strategy is not convenient to be implemented on the existing control system in our laboratory (Jiang et al., 2010). The reason is that the length of the time sequence would quite large and irregular, and it is therefore a big workload to type this time sequence into the existing control system before the fermentation. In what follow, we will present a problem specific time partition for the control function in (1) by using the empirical knowledge about the growth characteristic of the strain.

Firstly, according to the growth characteristic of the strain, the entire time horizon $[t_0, T]$ is divided into several phases by a main grid $t_0 = T_0 < T_1 < T_2 < \cdots < T_{N_T} = T$. Secondly, the subinterval $[T_{n-1}, T_n]$ is further divided into N_n units by introducing a minor grid

$$T_{n-1,j} := T_{n-1} + j \cdot dT_n, \quad j = 1, 2, \cdots, N_n,$$

where $dT_n = \dfrac{T_n - T_{n-1}}{N_n}$. Thirdly, in $[T_{n-1,j}, T_{n-1,j+1}]$, a glycerol input starts from the time $t = T_{n-1} + j \cdot dT_n$ and this input is stopped at some moment $t = T_{n-1} + j \cdot dT_n + \tau_n$, followed by a period of time without glycerol feeding until $t = T_{n-1} + (j+1) \cdot dT_n$. The partition of the time domain is illustrated in Figure 1.

Note that all the units $\{[T_{n-1,j}, T_{n-1,j+1}]\}_{j=1}^{N_n}$ in the phase $(T_{n-1}, T_n]$ have the same duration time for glycerol feeding. Obviously, $\tau_n \in [0, dT_n]$. For convenience, let $\tau := (\tau_1, \tau_2, \ldots, \tau_{N_T})^\intercal$, which is referred to as the glycerol switching signal vector. According to the above special time partition, the optimal control of glycerol feeding is equivalent to the optimization of the glycerol switching signal vector τ. The admissible set of τ is defined as $\Omega_{ad} := \prod_{n=1}^{N_T} [0, dT_n]$.

Remark 1. *The time partition in Figure 1 can be regarded as a special case of (1). In other words, it can be viewed as imposing a set of equality constraints in the time grids $\bar{b}_0, \bar{b}_1, \bar{b}_2, \cdots, \bar{b}_N$, where $\bar{b}_0 = T_0, \bar{b}_1 = T_0 + \tau_1, \bar{b}_2 = T_{0,1}, \bar{b}_3 = T_{0,1} + \tau_1, \bar{b}_4 = T_{0,2}, \cdots, \bar{b}_{2N_1} = T_{0,N_1}, \bar{b}_{2N_1+1} = T_{0,N_1} + \tau_2 = T_1 + \tau_2, \cdots, \bar{b}_N = T_N = T$ and $N = \sum_{n=1}^{N_T} 2N_n$. Correspondingly, the binary vector $\bar{a}$ in (1) is of the form $(F_G^m, 0, F_G^m, 0, \cdots)^\intercal$ with one dimension less than $\bar{b}$.*

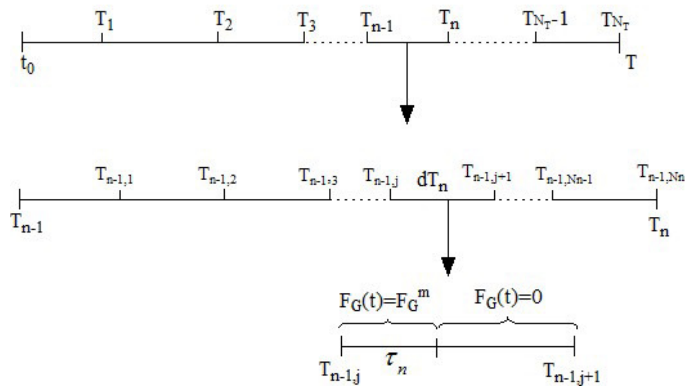

Figure 1: The illustration of time partition of the fed-batch culture.

Remark 2. *The special time partition here is given by the empirical knowledge of this particular fermentation process. In this context, the number of grid points N is a constant and therefore needn't be optimized. In addition, we can see in the later section that the number of continuous variables to be optimized, i.e., N_T, can also be greatly reduced by using the problem specific reformulation of glycerol input here compared with the general time partition in (1).*

2.2. Mathematical description of pH logic control process

According to the previous work (Ye et al., 2011), the pH value of the solution at time t is given by

$$\begin{aligned} ph(t) &= y_{\mathrm{pH}}(x(t)) \\ &= \begin{cases} pK_a - \log_{10} \frac{x_4 - \gamma x_6}{\gamma x_6} & \text{if } x_6 \geq \epsilon_0, \\ -\log_{10}\left(\frac{-K_a + \sqrt{K_a^2 + 4K_a x_4/(1000\gamma)}}{2} + \sqrt{K_w^-} \right) & \text{otherwise.} \end{cases} \end{aligned} \tag{2}$$

Here K_a is the averaged dissociation constant of acid byproducts, and $pK_a = -\log_{10}(K_a)$; $K_w^- = 1 \times 10^{-14}$ is the dissociation constant of water; γ is the ratio of acetic acid concentration to the total acid byproducts concentration; ϵ_0 is a sufficient small constant, below which the concentration of NaOH can be ignored while computing the pH.

According to the growth characteristic of the strain, the pH of the solution should be limited in a desired range $[\mathrm{pH}_*, \mathrm{pH}^*]$, which is described by the following inequality constraints.

$$ph_0(x(t)) := \mathrm{pH}^* - y_{\mathrm{pH}}(x(t)) \geq 0, \tag{3}$$

$$ph_1(x(t)) := y_{\mathrm{pH}}(x(t)) - \mathrm{pH}_* \geq 0. \tag{4}$$

Let $F_N(\cdot) : [t_0, T] \to \{0, F_N^m\}$ be a piecewise constant function representing the flow rate of alkali input, where $F_N^m > 0$ is the maximum flow rate of alkali solution. In detail, $F_N(t)$ takes value F_N^m when the alkali pump is on, and 0 otherwise. When $F_N(t) = F_N^m$ and $ph_0(x(t)) = 0$, it means that the pH reaches its allowable upper bound but the alkali flow is still kept feeding, so the pH control system will impose the alkali pump to be shut down. Alternatively, $F_N(t) = 0$ and $ph_1(x(t)) = 0$ implies that the pH reaches its allowable lower bound but the the alkali pump is still closed. The alkali pump is imposed to pour the alkali solution into the reactor in this situation until the pH value increases to its upper bound again. The process is repeated until the end of the fermentation. As a result, the function $F_N(\cdot)$ is naturally defined as follows.

$$\begin{cases} \dot{F}_N(t) = 0, & \text{if } ph_i(x(t)) \neq 0, i = 0, 1, \\ F_N(t^+) = i \cdot F_N^m, & \text{if } ph_i(x(t)) = 0, i \in \{0, 1\}, \\ F_N(t_0) = 0. \end{cases} \tag{5}$$

2.3. Nonlinear hybrid dynamical system in fed-batch culture

In the previous two subsections we developed formulations describing on/off switches of the pumps of glycerol and alkali, respectively. Let $f(x, F_G, F_N) := (f_1(x, F_G, F_N), f_2(x, F_G, F_N), \ldots, f_7(x, F_G, F_N))^\intercal$ be the vector field describing the temporal changes of the states during the fermentation process, the components of which are defined as follows referring to Ye et al. (2011).

$$f_1(x,F_G,F_N) = (\mu - d_s)x_1 - \frac{F_G(t)+F_N(t)}{x_7}x_1, \tag{6}$$

$$f_2(x,F_G,F_N) = -p_2x_1 + \frac{F_G(t)}{x_7}(C_{s_0} - x_2) - \frac{F_N(t)}{x_7}x_2, \tag{7}$$

$$f_k(x,F_G,F_N) = p_kx_1 - \frac{F_G(t)+F_N(t)}{x_7}x_3, k = 3,4,5, \tag{8}$$

$$f_6(x,F_G,F_N) = -\frac{F_G(t)}{x_7}x_6 + \frac{F_N(t)}{x_7}(\varrho - x_6), \tag{9}$$

$$f_7(x,F_G,F_N) = F_G(t) + F_N(t), \tag{10}$$

where $F_G(t)$ and $F_N(t)$ are defined in (1) and (5), respectively. d_s is the specific decay rate of cells. C_{s_0} (mmol·L^{-1}) and ϱ (mmol·L^{-1}) are the concentrations of glycerol and NaOH in feed medium, respectively. μ, p_2 and p_i, $k = 3,4,5$, are, respectively, the specific growth rate of cells, the specific consumption rate of glycerol and the specific formation rate of 1,3-PD, acetic acid and ethanol, which are given as follows.

$$\mu = \begin{cases} \mu_m \dfrac{x_2}{x_2+k_s}(1-\frac{x_1}{x_1^*})(1-\frac{x_2}{x_2^*})(1-\frac{x_3}{x_3^*})(1-\frac{x_4}{x_4^*})(1-\frac{x_5}{x_5^*}), \\ \quad \text{if } 0 < x_i \leq x_i^*, i = 1,2,3,4,5, \\ 0, \quad \text{otherwise}, \end{cases} \tag{11}$$

$$p_2 = m_2 + \frac{\mu}{Y_2} + \Delta_2\frac{x_2}{x_2+K_2^*}, \tag{12}$$

$$p_3 = m_3 + \mu Y_3 + \Delta_3\frac{x_2}{x_2+K_3^*}, \tag{13}$$

$$p_4 = m_4 + \mu Y_4 + \Delta_4\frac{x_2}{x_2+K_4^*}, \tag{14}$$

$$p_5 = m_5 + \mu Y_5 + \Delta_5\frac{x_2}{x_2+K_5^*}. \tag{15}$$

In (11)-(15), μ_m, k_s, m_i, Y_i, Δ_i and K_i^*, $i = 2,3,4,5$, are kinetic parameters; x_1^* is the carrying capacity of the reactor and x_i^*, $i = 2,3,4,5$, are respectively the critical concentrations of glycerol, 1,3-PD, acetic acid and ethanol for cell growth. The admissible set of the state vector x is defined as $W_{ad} := \prod_{i=1}^{7}[x_{i*}, x_i^*] \subset \mathbb{R}_+^7$, where x_6^* and x_7^* are the upper bounds of x_6 and x_7, and x_{i*}, $i = 1,2,\ldots,7$ are the lower bounds of x_i, respectively.

Based on the above definitions and notations, the fed-batch fermentation of glycerol can be described by

$$\begin{cases} \dot{x}(t) = f(x(t), F_G(t), F_N(t)), \\ x(t_0) = x^0, \end{cases} \tag{16}$$

Note that in the system (16), both the functions $F_G(t)$ and $F_N(t)$ take discrete values. The function $F_G(t)$ is explicitly defined by a piecewise constant function, and $F_N(t)$ is governed by the impulsive system (5), which is coupled with the system (16) since the continuous state is involved. Therefore, the entirety of (1), (5) and (16) is a hybrid dynamical system, which is referred to as the system HDS in the sequel.

According to the actual experiments, we make the following assumptions.

(H1) The concentrations of reactants are uniform in reactor, while time delay and nonuniform space distribution are ignored.

(H2) The substrates added to the reactor only include glycerol and alkali.

(H3) There exists a constant $C > 0$ such that, for all $x \in W_{ad}$,

$$\nabla ph_1(x) \cdot f(x, F_G, 0) \le -C, \quad \forall F_G \in \{0, F_G^m\},$$

and

$$\nabla ph_0(x) \cdot f(x, F_G, F_N^m) \le -C, \quad \forall F_G \in \{0, F_G^m\}.$$

Assumptions (H1) and (H2) are standard hypotheses in plenty of literature on modelling of reactor dynamics. On the other hand, the physical meaning of the assumption (H3) is that the change rate of the pH in the solution is bounded, which may be hard to be verified from the mathematical model, but an acceptable hypothesis from engineering point of view.

The solution of the system HDS is governed by several different vector fields depended on the different values of F_G and F_N. In detail, the system HDS will switch from one vector field to another if one of the following four conditions holds:

- $t - (T_{n-1} + j \cdot dT_n) = 0$ for some $n \in I_{N_T} = \{1, 2, \cdots, N_T\}$ and $j \in \bar{I}_{N_n - 1} = \{0, 1, 2, \cdots, N_n - 1\}$;

- $t-(T_{n-1}+j\cdot dT_n+\tau_n)=0$ for some $n\in I_{N_T}$ and $j\in \bar{I}_{N_n-1}$;
- $ph_0(x(t))=0$;
- $ph_1(x(t))=0$.

The above conditions determine the switching of the system HDS, which are referred to as the switching conditions of the system HDS. For convenience, the kth active switching condition is denoted as

$$g_{k+1}^{k}(t,x(t),\tau)=0. \tag{17}$$

Here, g_{k+1}^{k} is referred to as the discontinuity function of the kth continuous evolution.

Under the assumptions (H1)-(H3), we can obtain the following properties of the system HDS referring to the previous work (Ye et al., 2011).

Property 1. *Under the assumptions (H1)-(H3), the system HDS is non-Zeno for all $(\tau,T)\in\Omega_{ad}\times T_{ad}$ and $x^0\in W_{ad}$, i.e., the discrete variables $F_G(t)$ and $F_N(t)$ have at most finitely many times of switches over the time interval $[t_0,T]$. Furthermore, the system HDS has a unique solution with each pair (τ,T), denoted by $x(\cdot;\tau,T)$, which is continuous in (τ,T) on $\Omega_{ad}\times T_{ad}$.*

3. Optimal control of the nonlinear hybrid system

In the fed-batch culture, the set of decision variables are the glycerol switching signal vector τ and the terminal time T. The switching of the discrete variable $F_G(t)$ is explicitly determined by τ, while the switching of $F_N(t)$ depends on the state of the system, which is also indirectly affected by the τ. In the sequel, given τ and T, let $N_*^{\tau,T}<\infty$ be the total number of switches that the two discrete variables of the system HDS experiences over the interval $[t_0,T]$, and denote the switching instants by $t_1^\tau,t_2^\tau,\ldots,t_{N_*^{\tau,T}}^\tau$. For convenience, we set $t_0^\tau:=t_0$ and $t_{N_*^{\tau,T}+1}^\tau:=T$.

3.1. Optimal control problem and its properties

The optimal control problem is to find a feasible pair (τ, T) to maximize the productivity of 1,3-PD. For convenience, let $u := (\tau, T)$ and $\mathcal{U}_{ad} := \Omega_{ad} \times T_{ad}$. Then the optimal control problem can be formulated as

$$\text{(OCP)} \qquad \min_{u} \quad \mathcal{J}(u) := -x_3(T; u)/T$$

$$\text{s.t.} \quad x(t; u) \in W_{ad}, \ t \in [t_0, T], \tag{18}$$

$$x_3(T; u) \geq \bar{x}_3, \tag{19}$$

$$u \in \mathcal{U}_{ad}. \tag{20}$$

The constraint (19) is imposed to avoid the case that the optimal solution would be obtained when the biomass is still at the exponential growth stage and the concentration of 1,3-PD is relatively low. So, $\bar{x}_3$ is a preassigned lower bound of 1,3-PD.

To explicitly represent the inequality path constraint (18), we define the following functions.

$$\phi_i(x(t; u)) := x_i(t; u) - x_i^*,$$

$$\phi_{i+7}(x(t; u)) := x_{i*} - x_i(t; u) \quad i = 1, 2, \ldots, 7.$$

Then the inequality path constraint (18) can be rewritten as

$$\phi_i(x(t; u)) \leq 0, \quad \forall t \in [t_0, T], i \in I_{14}. \tag{21}$$

The existence of inequality path constraints would increase the complexity of the solution to the optimal control problem due to the potential high-index DAEs composed of the active path constraints and the original ODEs or DAEs. The existing methods for handling inequality path constraints can be classified into four broad categories: introducing squares of slack variables, addition of a penalty function to the objective function, using the penalty function to form a set of end-point constraints, and imposing pointwise constraints. Kameswaran and Biegler (2008) presented an excellent review on various methods for handling the inequality path constraints. In the control parametrization scheme, Feehery and Barton (1998, 1999) propose an algorithm for inequality path constraints (possibly high index) by detecting activation and deactivation of the constraints during the solution of the IVP and solving the resulting high index DAEs based on the method of dummy derivatives. However, for the particular problem considered in this work, since the decision variables are time-invariant parameters, which do not appear in the path constraints or the vector field, the approach proposed by Feehery and Barton (1999) cannot be applied.

The method adopt in this work is to transform the inequality path constraints into equivalent end-point constraints. One can refer to the previous work by Vassiliadis et al. (1994) for a detailed description of this method. For the particular problem (OCP), we can define a group of new differential variables φ_i, $i = 1, 2, \ldots, 14$, which are given by the following differential equations

$$\dot{\varphi}_i = (\max\{0, \phi_i(x(t; u))\})^2, t \in (t_k^\tau, t_{k+1}^\tau], k = 0, 1, \ldots, N_*^{\tau,T}, \tag{22}$$

with the initial condition

$$\varphi_i(t_0) = 0 \tag{23}$$

and junction conditions

$$\varphi_i(t_k^\tau +) = \varphi_i(t_k^\tau), k = 1, \ldots, N_*^{\tau,T}. \tag{24}$$

The path constraint (18) is equivalent to the end-point constraints

$$\varphi_i(T; u) = 0, i \in I_{14}. \tag{25}$$

A major disadvantage arising from the use of the end-point constraints (25) is that both the violation measure and its gradient with respect to all optimization parameters are zero when the constraint is inactive. Thus, no useful information can be conveyed to the optimizer regarding the proximity of the current point to the boundary of the feasible region, which may result in inefficient behavior involving excessive oscillations between feasible and infeasible choices of the optimization parameters in successive optimization steps or during the line-search procedure.

To overcome this problem, Walsh (1993) introduced a small violation tolerance $\epsilon > 0$ to the end-point equality constraints, resulting in the following inequality end-point constraints.

$$\varphi_i(T; u) \leq \epsilon, i \in I_{14}.$$

It was reported that the above relaxation of the path constraints could in general lead to significant performance improvement in the numerical computation (Vassiliadis et al., 1994). The problem (OCP) is finally approximated by

$$
\begin{aligned}
(\mathrm{OCP}_\epsilon) \qquad & \min_u \ \mathcal{J}(u) := -x_3(T; u)/T \\
& \text{s.t.} \ \varphi_i(T; u) \leq \epsilon, \ i \in I_{14}, \\
& \qquad \bar{x}_3 - x_3(T; u) \leq 0, \\
& \qquad u \in \mathcal{U}_{ad}.
\end{aligned}
$$

From Property 1 and (22)-(24), we can verify that φ_i, $i \in I_{14}$, are continuous in u on $\mathcal{U}_{ad}$, and readily obtain the following relationship between the solutions of the problem (OCP) and the problem (OCP$_\epsilon$) as $\epsilon \to 0$.

Property 2. *Let $\{u_\epsilon^*\}$ be a sequence of optimal solutions to (OCP$_\epsilon$) as $\epsilon \to 0$. Then there exists a subsequence of $\{u_\epsilon^*\}$ converging to a point $u^* \in \mathcal{U}_{ad}$, which is an optimal solution of the problem (OCP).*

Proof. The proof of the property is similar to that of Lemma 3.1 in Teo and Jennings (1989b). □

Property 2 indicates that the solution to the problem (OCP) can be approximately computed by solving a sequence of problems $\{(\mathrm{OCP}_\epsilon)\}$. Next, we shall derive the gradients of the cost functional and the constraints for the problem (OCP$_\epsilon$), and construct an algorithm to solve (OCP$_\epsilon$).

3.2. Parametric sensitivity functions and gradient information

To get the gradients of the cost functional and the constraints with respect to the decision variables, we shall first present the parametric sensitivity function for the system HDS.

The partial derivatives of the continuous state x with respect to the decision variables τ_n, $n = 1, 2, \ldots, N_T$, and T are referred to as parametric sensitivity functions. For convenience, we let $S_n(t; u) := \dfrac{\partial x(t; u)}{\partial \tau_n}$, $n = 1, 2, \ldots, N_T$, if the partial derivatives exist. In an abuse of notations, we use $f(t_k^\tau+)$ to denote $f(x(t_k^\tau+), F_G(t_k^\tau+), F_N(t_k^\tau+))$, and $f(t_k^\tau-)$ to denote $f(x(t_k^\tau-), F_G(t_k^\tau-), F_N(t_k^\tau-))$ for all $k = 1, 2, \cdots, N_*^{\tau,T}$.

Property 3. *(The parametric sensitivity function of x with respect to τ)*

Given $u \in \mathcal{U}_{ad}$, let $x(\cdot; u)$ be the solution of the system HDS over $[t_0, T]$. Assume that $x(t; u) \in \mathbb{R}_+^7$ for all $t \in [t_0, T]$, and assume that the following equations

$$\frac{\partial g_{k+1}^k}{\partial x} \mid_{t=t_k^\tau} f(t_k^\tau-) + \frac{\partial g_{k+1}^k}{\partial t} \mid_{t=t_k^\tau} \neq 0,$$

hold for all $k \in \{1, 2, \ldots, N_*^{\tau,T}\}$. Then, under the assumptions (H1)-(H3), the partial derivatives $S_n(t; u)$, $n = 1, 2, \ldots, N_T$, exist for all $t \neq t_k^\tau$ and satisfy the following equations

$$\frac{dS_n}{dt} = \frac{\partial f}{\partial x} S_n, \quad t_{k-1}^\tau < t \leq t_k^\tau, k = 1, 2, \ldots, N_*^{\tau,T} + 1, \tag{26}$$

with the initial conditions

$$S_n(t_0; u) = 0. \tag{27}$$

Moreover, the transition from one equation in (26) to another is given by

$$\triangle S_n(t_k^\tau) = (f(t_k^\tau-) - f(t_k^\tau+)) \frac{dt}{d\tau_n}, \tag{28}$$

for all $k \in \{1, 2, \ldots, N_*^{\tau,T}\}$, where

$$\triangle S_n(t_k^\tau) \triangleq S_n(t_k^\tau+; u) - S_n(t_k^\tau; u),$$

and

$$\frac{dt}{d\tau_n} = -\frac{\dfrac{\partial g_{k+1}^k}{\partial x} \mid_{t=t_k^\tau} S_n(t_k^\tau; u) + \dfrac{\partial g_{k+1}^k}{\partial \tau_n} \mid_{t=t_k^\tau}}{\dfrac{\partial g_{k+1}^k}{\partial x} \mid_{t=t_k^\tau} f(t_k^\tau-) + \dfrac{\partial g_{k+1}^k}{\partial t} \mid_{t=t_k^\tau}}. \tag{29}$$

Proof. From Eqs.(6)-(15), we can obtain that the function f is continuously differentiable with respect to x on $\mathbb{R}^7_+$. Then the conclusion of the theorem can be directly obtained by applying Theorem 3.1 in Rosenwasser and Yusupov (2000). $\square$

Note that the cost functional is of the form $\mathcal{J}(u) = -x_3(T;u)/T$. So the partial derivatives of the cost functional with respect to the decision variables τ_n, $n = 1, 2, \ldots, N_T$ can be readily obtained from Property 3. And its partial derivative with respect to T can be computed due to the fact

$$\frac{\partial x}{\partial T}(T;u) = \frac{dx}{dt}(T;u) = f(x(T;u), q_1(T;\tau), q_2(T)).$$

In addition, analogous to the proof of the above theorems, we can derive the partial derivatives of the constraint function φ_i $(i \in I_{14})$ with respect to τ_n $(n \in I_{N_T})$ as follows.

Property 4. *Under the assumptions (H1)-(H3), the partial derivative of the constraint function φ_i ($i \in I_{14}$) defined in (22)-(24) with respect to τ_n ($n \in I_{N_T}$), $\partial\varphi_i/\partial\tau_n$, exists for all $t \neq t_k^\tau$ and satisfies the following equations*

$$\frac{d}{dt}\left(\frac{\partial \varphi_i}{\partial \tau_n}\right) = 2\max\{0, \phi_i(t, x(t;u))\}\frac{\partial \phi_i}{\partial x}S_n, \quad t_{k-1}^\tau < t \leq t_k^\tau, \\ k = 1, 2, \ldots, N_*^{\tau,T} + 1, \tag{30}$$

with the initial condition

$$\frac{\partial \varphi_i}{\partial \tau_n}(t_0;u) = 0 \tag{31}$$

and junction condition

$$\frac{\partial \varphi_i}{\partial \tau_n}(t_k^\tau +) = \frac{\partial \varphi_i}{\partial \tau_n}(t_k^\tau). \tag{32}$$

Property 5. *The partial derivatives of the constraint function φ_i ($i \in I_{14}$) defined in (22)-(24) with respect to T, $\frac{\partial \varphi_i}{\partial T}$, exists for all $t \neq t_k^\tau$, taking values of zero except for the instant $t = T$, at which the following equation is satisfied.*

$$\frac{\partial \varphi_i}{\partial T}(T) = (\max\{0, \phi_i(x(T;u))\})^2, i \in I_{14}. \tag{33}$$

4. Optimization algorithm

In (OCP_ϵ), the variables to be optimized are the glycerol switching signal τ and the terminal time T. The problem is therefore an OPSP of switching system. On the other hand, note that the glycerol switching signal τ is in essential a scaled vector of model stage lengths. It was pointed out by Sager (2009a) that dynamic optimization of switching systems with variables of this kind may suffer several drawbacks: a nonregular situation may occur when state lengths are reduced to zero during optimization procedure, resulting in variable structures in the sensitivity system; the number of switches may be not known, left alone the precise switching structure; the reformulation yields additional nonconvexities in the optimization space. The above drawbacks are carefully treated in this work as follows. Firstly, to handle the problem that the stage lengths may be reduced to zero, we need to detect this special case during the optimization procedure. Whenever this nonregular case occurs, the structure of the switching system will be updated and the parametric sensitivity functions will be recomputed. Secondly, since the time horizon has been partitioned into a special structure as stated in Subsection 2.1, the maximum number of switches is known in advance. The number of switches decreases only when some stage length is reduced to zero, which has been discussed in the first case. Thirdly, the nonconvexities is a generic properties arising from the discrete valued of the control function. Although some sophisticated techniques have been developed for the convexification of this class of problems (e.g., Singer and Barton, 2006; Sahlodin and Chachuat, 2011), the efficient solution in this scheme still remains a daunting challenge for complicated or large scale problems, and many research areas still remain open for finding the global solution of complicated non-convex optimization problems (Singer and Barton, 2006). It is therefore not suggested to use the convexification techniques in many practical problems. Actually, a "good" local solution is often enough for most practical problems, rather than a global optimal one.

In finding the local solution of OPSPs, several successful families of algorithms have been developed (see, for example, Teo and Jennings, 1989b; Goh and Teo, 1988b; Polak and He, 1991; Polak, 1997). Generally, this class of problems can be solved by several common NLP algorithms (coupled with an appropriate ODE solver for evaluating the states and the sensitivity functions), such as penalty methods, augmented Lagrangian methods, sequential quadratic programming (SQP) methods, etc. It is well recognized that the performances of penalty and augmented Lagrangian methods are greatly affected by the update strategies of penalty factors and Lagrange multipliers, respectively. Even if a good update strategy for penalty factors or Lagrange multipliers is applied, there are a sequence of approximated problems parametrized by the penalty factors or Lagrange multipliers to be solved. The computation cost in the framework of penalty and augmented Lagrangian methods would be quite expensive, because differential systems and the sensitivity systems must be performed many times for each problem with fixed multiplier. On the other hand, the standard SQP methods require the solution of a general (inequality constrained) quadratic problem at each iteration. However, the evaluation of the Hessian would be computational expensive, in particular in dealing with the optimal control problem of switching systems. Because of the above considerations, we use the phase I-phase II method to solve (OCP_ϵ), because this method has good convergence results as shown in Polak (1997), while only the gradient information is required in the implementation of the algorithm.

To begin with, let

$$\begin{aligned}
&\varphi_i^\epsilon := \varphi_i(T,u) - \epsilon, i \in I_{14}\\
&\varphi_{15}^\epsilon := \bar{x}_3 - x_3(T;u),\\
&\Psi^\epsilon(T;u) := \max\{\varphi_i^\epsilon(T,u), i \in I_{15}\},\\
&\Psi_+^\epsilon(T;u) := \max\{0, \Psi^\epsilon(T;u)\}.
\end{aligned}$$

Let $\bar{\mathcal{J}} : \mathbb{R}^{N_T+1} \times \mathbb{R}^{N_T+1} \to \mathbb{R}$ be defined as

$$\bar{\mathcal{J}}^\epsilon(\bar{u},u) := \max\{\mathcal{J}(u) - \mathcal{J}(\bar{u}) - \lambda\Psi_+^\epsilon(T;\bar{u}), \Psi^\epsilon(T;u) - \Psi_+^\epsilon(T;\bar{u})\},$$

where $\lambda > 0$. Given $h \in \mathbb{R}^{N_T+1}$ and $\delta > 0$, let

$$\hat{\mathcal{J}}^\epsilon(u, u+h) := \max\{< \nabla_u \mathcal{J}(u), h > -\lambda\Psi^\epsilon_+(T; u), \max_{i\in I_{15}}\{\varphi^\epsilon_i(T; u) - \Psi^\epsilon_+(T; u) + < \nabla_u \varphi_i(T; u), h >\}\} + \frac{1}{2}\delta\|h\|^2$$

Note that $\hat{\mathcal{J}}^\epsilon(u, u+h)$ is a first-order, convex (in h) approximation to $\bar{\mathcal{J}}^\epsilon(u, u+h)$. Now we define the optimality function and descent direction for (OCP$_\epsilon$) as follows.

$$\theta^\epsilon(u) := \min_{h\in\mathbb{R}^{N_T+1}} \hat{\mathcal{J}}^\epsilon(u, u+h), \tag{34}$$

$$h(u) := \arg \min_{h\in\mathbb{R}^{N_T+1}} \hat{\mathcal{J}}^\epsilon(u, u+h). \tag{35}$$

According to Theorem 2.2.8 in Polak (1997), $\theta^\epsilon(u)$ and $h(u)$ are given by

$$\theta^\epsilon(u) = -\min_{\eta\in\Sigma^0_{15}} \{\eta_0\lambda\Psi^\epsilon_+(u) + \sum_{i=1}^{15} \eta_i(\Psi^\epsilon_+(u) - \varphi^\epsilon_i(T; u)) + \frac{1}{2\delta}\|\eta_0\nabla_u\mathcal{J}(u) + \sum_{i=1}^{15} \eta_i\nabla_u\varphi_i(T; u)\|^2\}, \tag{36}$$

$$h(u) = -\frac{1}{\delta}(\eta^u_0\nabla_u\mathcal{J}(u) + \sum_{i=1}^{15} \eta^u_i\nabla_u\varphi_i(T; u)), \tag{37}$$

where $\eta := (\eta_0, \eta_1, \cdots, \eta_{15})^\intercal$, $\Sigma^0_{15} := \{\eta \in \mathbb{R}^{16} \mid \sum_{i=0}^{15} \eta_i = 1, \eta_i \geq 0, i = 0, 1, \ldots, 15\}$ and η^u is a solution of (36). Let $\bar{\xi} = (\xi^0, \xi^\intercal)^\intercal$ with $\xi^0 \in \mathbb{R}$ and $\xi \in \mathbb{R}^{N_T+1}$, and let

$$GJ^\epsilon(u) = \mathrm{co}\left\{\begin{pmatrix} \lambda\Psi^\epsilon_+(T; u) \\ \nabla_u\mathcal{J}(u) \end{pmatrix}, \begin{pmatrix} \Psi^\epsilon_+(T; u) - \varphi^\epsilon_i(T; u) \\ \nabla_u\varphi_i(T; u) \end{pmatrix}, i \in I_{15}\right\}. \tag{38}$$

Then $\theta^\epsilon(u)$ and $h(u)$ can be equivalently expressed in the form

$$\theta^\epsilon(u) \quad = \quad -\min_{\bar{\xi}\in GJ^\epsilon(u)}\{\xi^0 + \frac{1}{2\delta}\|\xi\|^2\}, \tag{39}$$

$$\bar{h}^\epsilon(u) \quad = \quad (h^{0,\epsilon}(u), h^\intercal(u))^\intercal = -\arg\min_{\bar{\xi}\in GJ^\epsilon(u)}\{\xi^0 + \frac{1}{2\delta}\|\xi\|^2\}. \tag{40}$$

We construct the following algorithm for solving (OCP$_\epsilon$).

Algorithm 4.1

Step 1. Set $\alpha \in (0,1]$, $\beta \in (0,1)$, $\lambda, \delta > 0$, $M \in \mathbb{Z}_+$, $0 < \varepsilon_0 \ll 1$, $k = 0$, $u^0 \in \mathcal{U}_{ad}$.

Step 2. At $u := u^k$, solve the system HDS, compute the parameter sensitivity functions defined in (26)-(29), the transformed constraint functions defined in (22)-(24), and the related gradients from (30)-(32) and (33), respectively.

Step 3. Solve the problem (39) at $u = u^k$. Set $\theta^k := \theta^\epsilon(u^k)$, $\bar{h}^k := \bar{h}^\epsilon(u^k) = (h^{0,\epsilon}(u^k), h^\intercal(u^k))^\intercal$ and $h^k := h(u^k)$. If $\theta^k > -\varepsilon_0$, stop; else goto Step 4.

Step 4. Set the stepsize

$$\iota^k := \max_{i \in \bar{I}_M} \{\beta^i \mid \hat{\mathcal{J}}(u^k, u^k + \beta^i h^k) \le \beta^i \alpha \theta^k\}.$$

Step 5. Set $u^{k+1} := u^k + \iota^k h^k$, replace k by $k+1$, and goto Step 2.

In algorithm 4.1, the parameter ε_0 defines the precision of the conceptual stopping criterion $\theta^\epsilon(u) = 0$. The set $\bar{I}_M$ in Step 4 is defined as

$$\bar{I}_M := \{0, 1, 2, \cdots, M\},$$

where β^M is the minimum stepsize.

In the kth iteration of Algorithm 4.1, the problem (39) can be numerically solved by the following subprocedure based on the Franke-Wolfe algorithm in Polak (1997).

Subprocedure 4.2

Step I-1. Set $\bar{\xi}^0 \in GJ^\epsilon(u^k)$, $0 < \varepsilon_1 \ll 1$, $\varpi^0 := \bar{\xi}^0$, $M_1 \in \mathbb{Z}_+$, $j = j_1 = 0$.

Step I-2. Compute

$$\bar{\zeta}^j := \arg\min\{< \nabla\Upsilon(\bar{\xi}^j), \bar{\zeta} - \bar{\xi}^j > | \bar{\zeta} \in GJ^\epsilon(u^k)\} \tag{41}$$

with $\Upsilon(\bar{\xi}) := \xi^0 + \frac{1}{2\delta}\|\xi\|^2$. Set $d\bar{\xi}^j := \bar{\zeta}^j - \bar{\xi}^j$ and goto Step I-3.

Step I-3. If ($j > 0$ and j mod M_1 =0), set $\varpi^{j_1} := \bar{\zeta}^j - \bar{\xi}^{j-M_1}$ and $j_1 := j_1 + 1$. If $\|\varpi^{j_1}\| \le \varepsilon_1$, stop; else goto Step I-4.

Step I-4. Compute the stepsize

$$\ell_j := \arg\min\{\Upsilon(\bar{\xi}^j + \ell \cdot d\bar{\xi}^j) | \ell \in [0,1]\}. \tag{42}$$

Set $\bar{\xi}^{j+1} := \bar{\xi}^j + \ell_j \cdot d\bar{\xi}^j$, replace j by $j+1$, and goto Step I-2.

Remark 3. *Note that the search direction finding problem (41) is a linear program, and hence, can be evaluated in a finite number of operations. In fact, it follows from the definition of $GJ^{\epsilon}(u^k)$ in (38) that solving (41) needs at most 16 inner product computations and a comparison of these inner products. In addition, the problem (42) can be solved by Golden Section Search method.*

Remark 4. *Generally, one can use $d\bar{\xi}^j \leq \varepsilon_1$ as the stop criterion for the Subprocedure 4.2. However, our numerical experiments show that the subprocedure may stop too early by using such criterion, which would reduce the performance of Algorithm 4.1. Therefore, we adopt $\varpi^{j_1} \leq \varepsilon_1$ as the stop criterion to avoid the possible premature termination of the subprocedure.*

5. Numerical results

The system HDS and the coupled parametric sensitivity systems need to be solved simultaneously. Compared with the numerical simulator for the system HDS in Ye et al. (2011), the computation of the parameter sensitivity systems requires much higher precision, because there exist intensive state-depended impulses in the parametric sensitivity systems. We use a novel alterative step Euler method to solve the systems. The solver is coded in Visual C++ 6.0. The values of the parameters and the critical values of the states of the system HDS are given in Table 1, which can also be referred to Ye et al.(2011). Figures 2 and 3 show, respectively, the trajectories of the sensitivity functions $\dfrac{\partial x_1}{\partial \tau_5}$ and $\dfrac{\partial x_3}{\partial \tau_5}$ with the initial state and glycerol switching signal vector given in Ye et al.(2011), where Figures 2(a) and 3(a) are the trajectories over the time interval [0,39], and Figures 2(b) and 3(b) are the corresponding partially enlarged views over the time interval [15,17.5], respectively.

Table 1: The values of parameters and the critical values of the states of the system HDS.

d	m_2	m_3	m_4	m_5	K_2^*	K_3^*	K_4^*	K_5^*
0.02	0	-6.325	-1.345	0.66	20.5	28.5	85.71	-
Y_2	Y_3	Y_4	Y_5	Δ_2	Δ_3	Δ_4	Δ_5	
0.008473	90.482	23.8599	2.66	9.5306	12.9	2.0099	-	
pH_*	pH^*	x_1^*	x_2^*	x_3^*	x_4^*	x_5^*	x_6^*	x_7^*
6.4	6.6	10	2039	1300	1026	360.9	500	5
x_{1*}	x_{2*}	x_{3*}	x_{4*}	x_{5*}	x_{6*}	x_{7*}		
0	0	0	0	0	0	2		

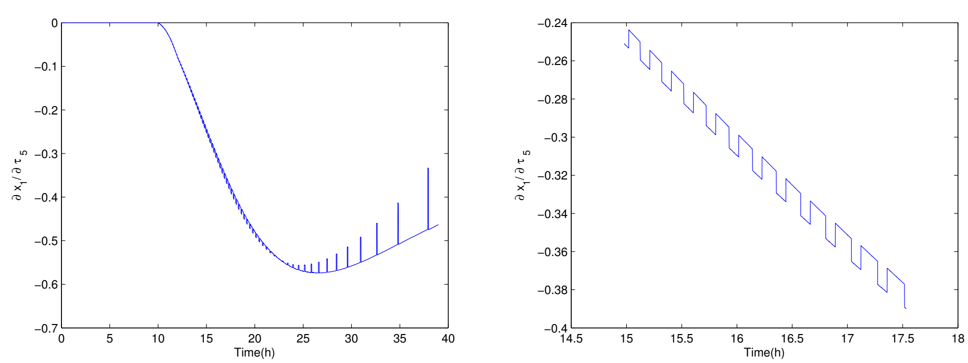

(a) The entire trajectory of $\frac{\partial x_1}{\partial \tau_5}$.

(b) The partially enlarged view of $\frac{\partial x_1}{\partial \tau_5}$.

Figure 2: The trajectory of $\frac{\partial x_1}{\partial \tau_5}$ over the time intervals [0,39] and [15,17.5].

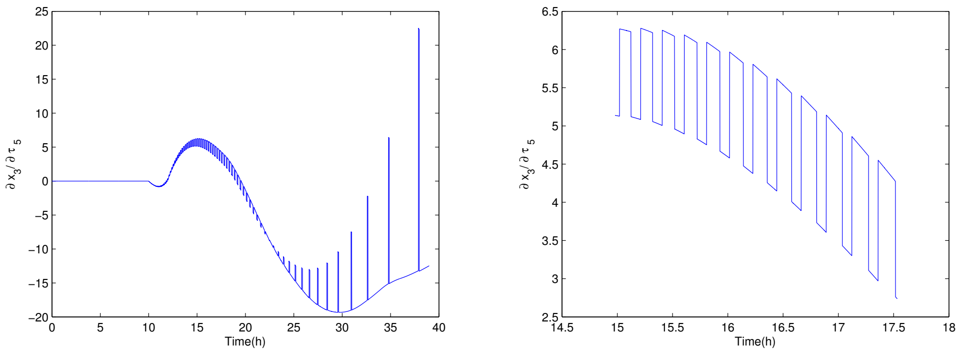

(a) The entire trajectory of $\frac{\partial x_3}{\partial \tau_5}$.　(b) The partially enlarged view of $\frac{\partial x_3}{\partial \tau_5}$.

Figure 3: The trajectory of $\frac{\partial x_3}{\partial \tau_5}$ over the time intervals [0,39] and [15,17.5].

In Algorithm 4.1 and Subprocedure 4.2, the parameters $\alpha, \beta, \lambda, \delta$, M, M_1, ε_0, ε_1 are, respectively, 0.8, 0.9, 3.0, 2.0, 25, 50, 0.005, 0.001. These parameters are derived empirically after numerous experiments. The violation tolerance ϵ is set to be 0.01.

For ease of calculation, the terminal time of the fermentation is preassigned as 45h. For each τ, the optimal terminal time T^*_τ can be easily calculated in the numerical simulation of the system HDS. Therefore, only τ needs to be optimized in Algorithm 4.1. According to the growth characteristics of the strain, the total fermentation time is divided into 26 phases. The start time of these phases are $0 < 3 < 5 < 6 < 7 < 8 < 9 < 10 < 10.5 < 11 < 12 < 13 < 14 < 15 < 18 < 20 < 22 < 24 < 26 < 28 < 30 < 32 < 34 < 36 < 39 < 42$. In addition, each phase is divided into several units with the same length $dT_n = 100$ (seconds), $n = 1, 2, \cdots, 26$.

The admissible set of τ, $\Omega_{ad} \subset \mathbb{R}^{26}_+$, is given on empirical basis. Algorithm 4.1 is run under different initial points, which are randomly generalized from Ω_{ad} (except for one initial point given based on the strategy in Ye et al.(2011)). The algorithm is performed in Visual C++ 6.0 on an Intel Core i5 with 2450GHz. The average iterations of the algorithm required to find the (local) optimal solution is calculated, and 17 runs failed to converge (60 runs in total) are excluded in the calculation of the average. The average iterations of the algorithm is about 167. The computational time of the run from which the optimal strategy is obtained is about 2.13h, and the average computational time of the successful runs is about 3.45h.

The optimal glycerol switching signal vector is $\tau^* = (0.00, 0.40, 0.51, 0.70, 0.48, 0.50, 0.48, 1.54, 2.24, 3.42, 1.25, 1.55, \ 1.65, 1.65, \ 1.62, \ 2.32, 1.77, 1.89, \ 1.23, 1.0, 0.76, 0.97, 1.58, 0.89, 0.8, 0.8)^\intercal$ (seconds), and the optimal terminal time under $\tau = \tau^*$ is $T^*_{\tau^*} = 14.9167$(h). Under the obtained optimal glycerol switching signal vector and the optimal terminal time, the productivity of 1,3-PD is 45.5342 (mmol$\cdot$ L$^{-1}\cdot$h^{-1}), which is increased by 53.1% in comparison with the experimental result presented in Ye et al. (2011).

The state trajectories of the system HDS and the trend of the performance index $x_3(t)/t$ with $\tau = \tau^*$ are shown in Figures 4-7. In addition, the change of the values of the binary function $q_2(t)$, which implies the occurrence of on/off switches of alkali pump, is depicted in Figures 8(a) and 8(b), where Figure 8(a) is a plot consisting of dots recoded at the discretization grids in the simulation of the system HDS, and Figure 8(b) is a line plot of part of these points. Figure 8(a) shows that the switching frequency of alkali pump decreases as time goes on, which is consistent with the fact that the formation rates of acid byproducts decrease with time. We also plot the trajectory of the discrete state $q(t)$ in Figures 9(a) and 9(b), which represent the order of the active operation modes as the fermentation goes on. Similarly, Figure 9(a) is a plot of dots and Figure 9(b) is a line plot. Here we do not plot the trajectories of $q_2(t)$ and $q(t)$ over the entire time horizon, because the values of the two functions change too frequently, resulting in poor view of the trajectories over the entire time horizon.

6. Discussions and conclusions

In this paper, an optimal control problem for the bioconversion of glycerol to 1,3-PD in fed-batch culture was considered, which is subject to inequality path constraints. Although the simultaneous approaches can deal with path

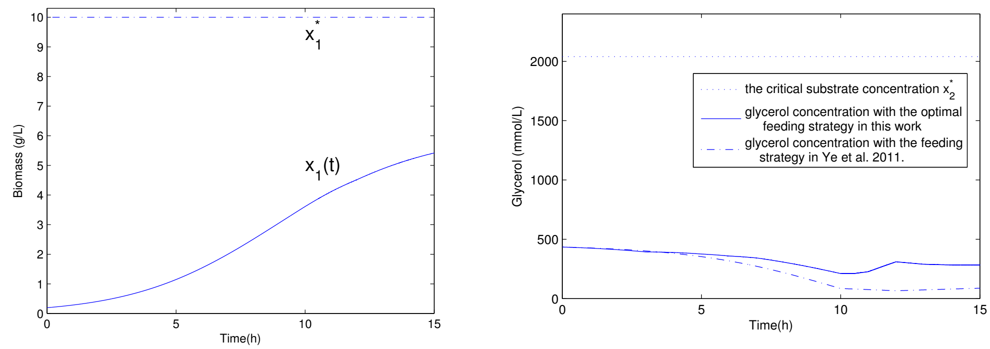

(a) (b)

Figure 4: (a) The trajectory of biomass concentration $x_1(t)$ with $\tau = \tau^*$ over the time horizon [0,T^*] and, (b) the trajectories of glycerol concentration $x_2(t)$ under different feeding strategies over the time horizon [0,T^*].

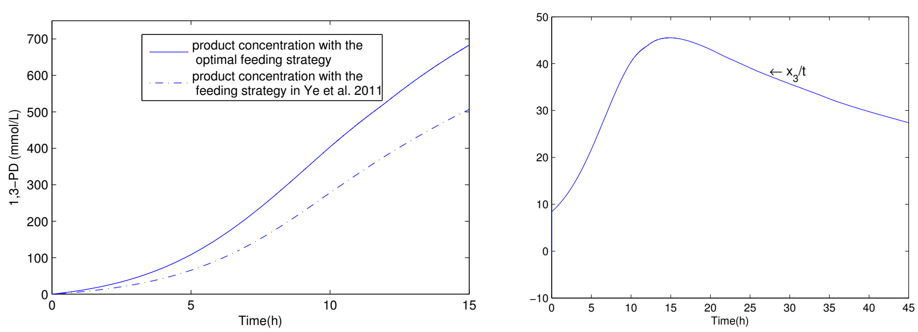

(a) (b)

Figure 5: (a) The trajectories of 1,3-PD concentration $x_3(t)$ under different feeding strategies over the time horizon [0,T^*] and, (b) the performance index $x_3(t)/t$ with $\tau = \tau^*$ over the time horizon [0,45].

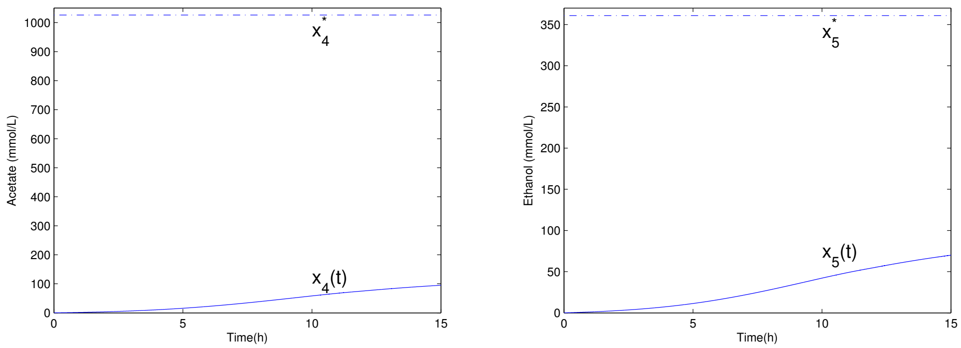

(a) (b)

Figure 6: (a) The trajectory of acetate concentration $x_4(t)$ with $\tau = \tau^*$ over the time horizon [0,T^*] and, (b) the trajectory of ethanol concentration $x_5(t)$ with $\tau = \tau^*$ over the time horizon [0,T^*].

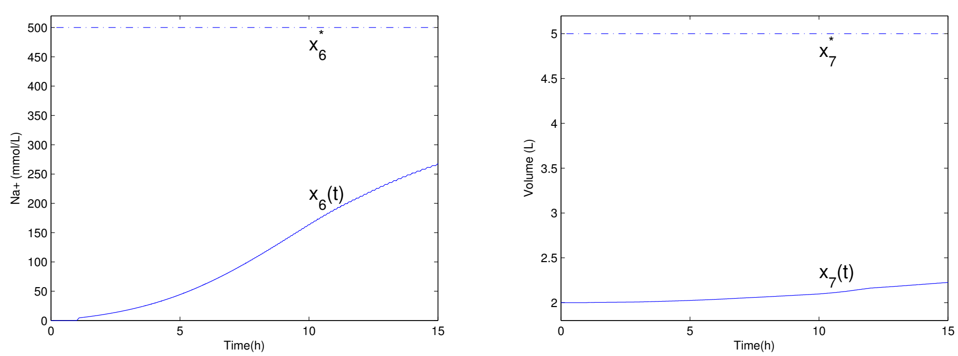

(a) (b)

Figure 7: (a) The trajectory of Na+ concentration $x_6(t)$ with $\tau = \tau^*$ over the time horizon [0,T^*] and, (b) the trajectory of the volume of the solution $x_7(t)$ with $\tau = \tau^*$ over the time horizon [0,T^*].

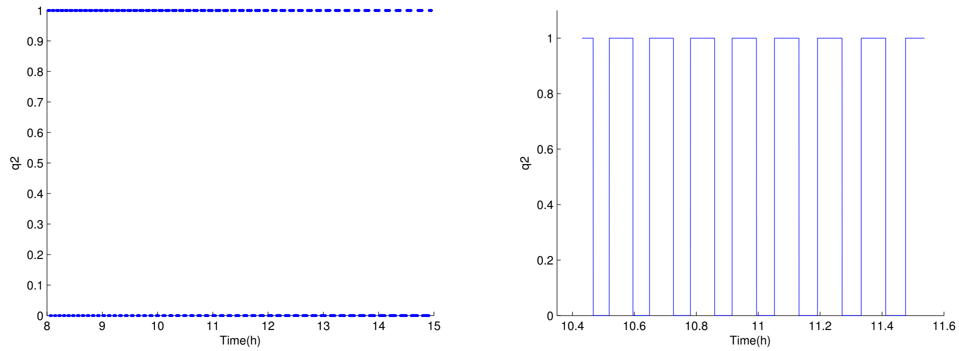

(a) (b)

Figure 8: (a) The trajectory of $q_2(t)$ plotted by dots with $\tau = \tau^*$ over the time horizon [8.0,14.9167] and, (b) the partially enlarged line plot of $q_2(t)$ with $\tau = \tau^*$ over the time horizon [10.4,11.5].

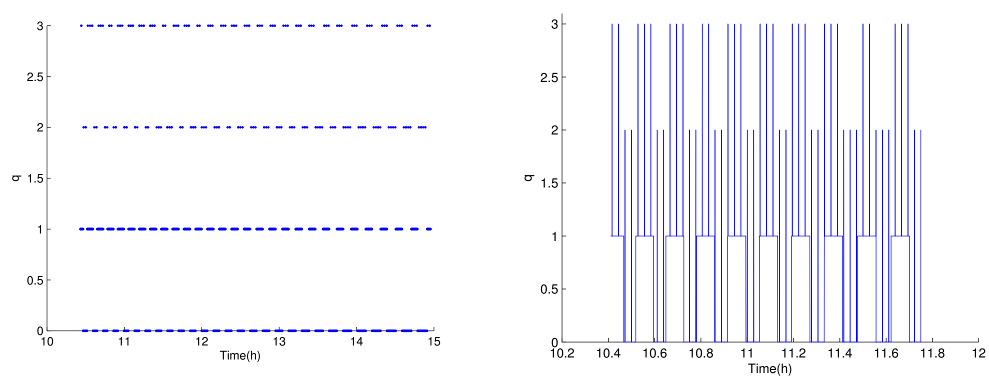

(a) (b)

Figure 9: (a) The trajectory of $q(t)$ plotted by dots with $\tau = \tau^*$ over the time horizon [10.4,14.9167] and, (b) the partially enlarged line plot of $q(t)$ with $\tau = \tau^*$ over the time horizon [10.4,11.75].

constraints efficiently, we didn't design optimization algorithm in this scheme. The reason is that the application of simultaneous approaches on this problem would greatly increase the size of the optimization problem. Alternatively, by employing the special time partition in this work, which is constructed in consideration of the growth characteristic of the strain, the variables to be optimized form only a finite dimensional control vector with small size. Numerical results reveal that the proposed algorithm can solve the optimal control problem efficiently, and that the productivity of 1,3-PD can be significantly improved by employing our optimal control strategy.

Comparing the glycerol concentration under the optimal feeding strategy with the strategy in previous work (Ye et al. 2011), we can find in Figure 4(b) that the curve of glycerol concentration in previous work has a more noticeable variance. It means that the substrate concentration is kept more stable under the optimal feeding strategy obtained in this work. Particularly, under the feeding strategy of previous work, the concentration of glycerol was too low after 5 hours of fermentation, which is disadvantageous for the growth of strains and limits the formation of the goal product. We can also see from Figure 5(a) that the concentration of the product with the optimal feeding strategy is considerable higher than that of previous work (Ye et al. 2011). On the other hand, we can see from Figure 8(a) that the switching frequency of alkali pump decreases as time goes on, which is consistent with the fact that the formation rates of acid byproducts decrease as time goes on.

Acknowledgements

This work is partially supported by National Natural Science Foundation of China (Grant Nos. 11301081, 11171050, 11171079, 61290325, 61321003), China Postdoctoral Science Foundation (Grant No. 2014M552027), Fujian Department of Education Technology Project (Grant No. JB12041), Provincial Natural Science Foundation of Fujian (Grant No. 2014J05001), HUST Startup Research Fund, and HUST Independent Innovation Research Fund (GF and

Natural Science).

The authors are grateful to the reviewers for constructive comments and suggestions.

References

Asenjo, J. A., Sun, W -H., Spencer, J. L. (1996). Optimal control of batch processes involving simultaneous enzymatic and microbial reactions. Bioprocess Eng. 14(6), 323-329.

Banga, J. R., Canto, E. B., Moles, C. G., Alonso, A. A. (2003). Dynamic optimization of bioreactors: A review. Proc. Indian Natl. Sci. Acad. 69, 257-265.

Banga, J. R., Canto, E. B., Moles, C. G., Alonso, A. A. (2005). Dynamic optimization of bioprocesses: efficient and robust numerical strategies. J. Biotechnol. 117(4):407-419.

Barton, P. I., Banga, J. R., Galan, S. (2000). Optimization of hybrid discrete: continuous dynamic systems. Comput. Chem. Eng. 24, 2171-2182.

Barton, P. I., Lee, C. K. (2002). Modelling, simulation, sensitivity analysis, and optimization of hybrid systems. ACM T. Model. Comput. S. 12, 256-289.

Biegler, L. T. (1984). Solution of dynamic optimization problems by successive quadratic programming and orthogonal collocation. Comput. Chem. Eng. 8(3/4), 243-248.

Biegler, L. T. (2007). An overview of simultaneous strategies for dynamic optimization. Chem. Eng. Process. 46, 1043-1053.

Bryson, A. E., Ho, Y. C. Applied optimal control. Hemisphere Publishing Corporation: New York, 1975.

Cacik, F., Dondo, R. G., Marques, D. (2001). Optimal control of a batch bioreactor for the production of xanthan gum. Comput. Chem. Eng. 25, 409-418.

Cheng, K. K., Sun, Y., Liu, W. B. (2004). Effect of feeding strategy on 1,3- propanediol fermentation with *Klebsiella* pneumoniae. Food & Fermentation Industries. 30(4), 1-5.

Chen, Theodore W.C. and Vassiliadis, V. S. (2005). Inequality path constraints in optimal control: a finite iteration ε-convergent scheme based on pointwise discretization. J. Process Contr. 15, 353-362.

Drag, P. and Styczen, K. (2012). Parallel simultaneous approach for optimal control of DAE systems. Proceeding of the Federated Conference on Computer Science and Information Systems. 517-523.

Egerstedt, M., Wardi, Y., Delmotte, F. (2003). Optimal control of switching times in switched dynamical systems. Proceeding of Conference on Decision and Control. 3, 2138-2143.

Feehery, W.F. and Barton, P. I. (1998). Dynamic optimization with state variable path constraints. Comput. Chem. Eng. 22, 1241-1256.

Feehery, W.F. and Barton, P. I. (1999). Dynamic optimization with equality path constraints. Ind. Eng. Chem. Res. 38, 2350-2363.

Gao, C. X., Li, K. Z., Feng, E. M., Xiu, Z. L. (2006). Nonlinear impulsive system of fed-batch culture in fermentative production and its properties. Chaos Soliton Fract. 28(1), 271-277.

Goh, C. J. and Teo, K. L. (1988a). Control parametrization: A unified approach to optimal control problems with general constraints. Automatica. 24, 3-18.

Goh, C. J. and Teo, K. L. (1988b). MISER: A FORTRAN program for solving optimal control problems. Adv. Eng. Soft. 10, 90.

Homann, T., Tag, C., Biebl, H., Deckwer, W.D., Schink, B. (1990). Fermentation of glycerol to 1,3-propanediol by *Klebsiella* and *Citrobacter* strains. Appl. Microbiol. Biotechnol. 33, 21-26.

Jiang, S., Ye, J. X., Feng, E. M., Xiu, Z. L. (2010). Automatic control design for optimal strategy in fed-batch culture with coupled feed of glycerol and alkali. Int. J. Chem. React. Eng. 8, Article A148.

Kameswaran, S. and Biegler, L.T (2008). Advantages of nonlinear-programming-based methodologies for inequality path constrained optimal control problems-A case study. SIAM J. Sci. Comput. 30(2): 957-981.

Leineweber, D. B., Schäfer, A., Bock, H. G., Schlöder, J. P. (2003a). An efficient multiple shooting based reduced SQP strategy for large scale dynamic process optimization Part I: theoretical aspects. Comput. Chem. Eng. 27, 157-166.

Leineweber, D. B., Schäfer, A., Bock, H. G., Schlöder, J. P. (2003b). An efficient multiple shooting based reduced SQP strategy for large scale dynamic process optimization Part II: Software aspects and applications. Comput. Chem. Eng. 27, 167-174.

Liu, C. Y., Gong, Z. H., Feng, E. M. (2011). Modeling and optimal control of a nonlinear dynamical system in microbial fed-batch fermentation. Math. Comput.

Model. 53(1-2), 168-178.

Logist, F., Van Erdeghem, P., Van Impe, J. (2009). Efficient deterministic multiple objective optimal control of (bio)chemical processes. Chem. Eng. Sci. 64, 2527-2538.

Logist, F., Telen, D., Houska, B., Diehl, M., Van Impe, J. (2013). Multi-objective optimal control of dynamic bioprocesses using ACADO Toolkit, Bioproc. and Biosyst. Eng. 36, 151-164.

Loxton, R. C., Teo, K. L., Rehbock, V., Ling, W. K. (2009). Optimal switching instants for a switched-capacitor DC/DC power converter. Automatica. 45, 973-980.

Mandli, A. and Modak, J. (2012). Evolutionary algorithm for the determination of optimal mode of bioreactor operation. Ind. Eng. Chem. Res. 51, 1796-1808.

Polak, E. and He, L. (1991). Unifed steerable phase I - phase II method of feasible directions for semi-infinite optimization. J. Optimiz. Theory App. 69, 83-107.

Polak, E. Optimization algorithm and consistent approximations. Springer, New York, 1997.

Renfro, J. G., Morshedi, A.M., Asbjornsen, O. A. (1987). Simultaneous optimization and solution of systems described DAEs. Comput. Chem. Eng. 11(5), 503-517.

Rosenwasser, E. and Yusupov, R. Sensitivity of automatic control systems. Tom Kurfess (ed). CRC Press, 2000.

Sager, S. (2009a). Reformulation and algorithms for the optimization of switching decisions in nonlinear optimal control. J. Process Contr. 19, 1238-1247.

Sahlodin, A.M., Chachuat, B. (2011). Discretize-then-relax approach for convex/concave relaxations of the solutions of parametric ODEs. Appl. Numer. Math. 61, 803-820.

Singer, A. B., Barton, P. I. (2006). Global optimization with nonlinear ordinary differential equations. J. Global Optim. 34, 159-190.

Tsang, T. H., Himmelblau, D. M., Edgar, T. F. (1975). Optimal control via collocation and nonlinear programming. Int. J. Control. 21, 763-768.

Teo, K. L., and Goh, C.J. (1989a). A computational method for combined optimal parameter selection and optimal control problems with general constraints. J. Austral. Math. Soc. Ser. B. 30, 350-364.

Teo, K. L., and Jennings, L. S. (1989b). Nonlinear optimal control problems with continuous state inequality constraints. J. Optimiz. Theory App. 63(1), 1-22.

Vassiliadis, V. S., Sargent, R. W. H., Pantelides, C.C. (1994). Solution of a class of multistage dynamic optimization problems. 2. Problems with path constraints. Ind. Eng. Chem. Res. 33, 2123-2133.

Wang, G., Feng, E. M., Xiu, Z. L. (2008). Modeling and parameter identification of microbial bioconversion in fed-batch cultures. J. Process Contr. 18, 458-464.

Wang, L., Ye, J. X., Yin, H. C., Feng, E. M., Wang, W. (2012a). Sensitivity analysis and identification of kinetic parameters in batch fermentation of glycerol. J. Comput. App. Math. 236, 2268-2276.

Wang, L., Xiu, Z. L., Gong, Z. H., Feng, E. M. (2012b). Modelling and parameter identification for multistage simulation of microbial bioconversion in batch culture. Int. J. Biomath. 5(4), 1250034 (12 pages).

Wang, L. (2012c). Modelling and regularity of nonlinear impulsive switching dynamical system in fed-batch culture. Abstr. Appl. Anal. doi:10.1155/2012/295627.

Walsh, S.P. (1993). Integrated design of chemical waste water treatment systems. Ph.D. thesis, University of London.

Xu, X.P. and Antsaklis P. J. (2002). Optimal control of switched systems via non-linear optimization based on direct differentiations of value functions. Int. J. Control. 75, 1406-1426.

Yan, H. H., Zhang, X., Ye, J. X., Feng, E. M. (2012). Identification and robustness analysis of nonlinear hybrid dynamical system concerning glycerol transport mechanism. Comput. Chem. Eng. 40, 171-180.

Ye, J. X., Feng, E. M., Yin, H. C., Xiu, Z. L. (2011). Modelling and well-posedness of a nonlinear hybrid system in fed-batch production of 1,3-propanediol with open loop glycerol input and pH logic control. Nonlinear Anal-Real. 12, 364-376.

Ye, J. X., Zhang, Y. D., Feng, E. M., Xiu, Z. L., Yin, H. C. (2012). Nonlinear hybrid system and parameter identification of microbial fed-batch culture with open loop glycerol input and pH logic control. Appl. Math. Model. 36, 357-369.

Zeng, A. P., Ross, A., Biebl, H., Tag, C., Günzel, B., Deckwer, W.D. (1994). Multiple product inhibition and growth modeling of Clostridium butyricum and Klebsiella pneumoniae in glycerol fermentation. Biotechnol. Bioeng. 44, 902-911.